

Lattice structure and magnetization of LaCoO_3 thin films

A. D. Rata^a, A. Herklotz, L. Schultz, and K. Dörr

IFW Dresden, Institute for Metallic Materials, Helmholtzstraße 20, 01069 Dresden, Germany

Received: date / Revised version: date

Abstract. We investigate the structure and magnetic properties of thin films of the LaCoO_3 compound. Thin films are deposited by pulsed laser deposition on various substrates in order to tune the strain from compressive to tensile. Single-phase (001) oriented LaCoO_3 layers were grown on all substrates despite large misfits. The tetragonal distortion of the films covers a wide range from -2% to 2.8% . Our LaCoO_3 films are ferromagnetic with Curie temperature around 85 K, contrary to the bulk. The total magnetic moment is below $1\mu_B/\text{Co}^{3+}$, a value relatively small for an excited spin-state of the Co^{3+} ions, but comparable to values reported in literature. A correlation of strain states and magnetic moment of Co^{3+} ions in LaCoO_3 thin films is observed.

PACS. 68.55.-a Thin film structure and morphology – 75.70.-i Magnetic properties of thin films, surfaces, and interfaces – 75.70.Ak Magnetic properties of monolayers and thin films

1 Introduction

The nature of the phase transition observed in LaCoO_3 compound from a nonmagnetic insulator at low temperatures to a paramagnetic semiconductor above 90 K has triggered tremendous experimental and theoretical efforts in the last years, see Refs. [1,2,3] and references therein. Recently, LaCoO_3 has attracted renewed interest due to the observation of ferromagnetism in thin films [4,5,6,7]. The bulk LaCoO_3 is nonmagnetic at low temperatures,

with Co^{3+} ions having low spin configuration ($S=0$). Contrary, the LaCoO_3 thin films grown on various substrates exhibit a ferromagnetic ground state below 85 K [5,6,7]. Regarding the origin of the observed ferromagnetism, several scenarios can be found in literature, *i.e.* Jahn-Teller distortions and the rotation of the CoO_6 octahedra, oxygen vacancies, increased volume and strain-enhanced ferromagnetism [4,6,7,8]. On the theoretical side, the findings are contradictory. Rondinelli *et al.* [9] found that strain-induced changes in lattice parameters are insuffi-

^a Corresponding author: email d.rata@ifw-dresden.de

cient to cause transitions to excited spin states of Co³⁺ ions at reasonable values of strain. Gupta *et al.* [11] recently indicated that the strain-induced pseudo-tetragonal structure is responsible for the spin-state transition in LaCoO₃. The authors of Ref. [11] observed that there is a very small CoO₆ angle dependence on strain, contrary to earlier suggestions. Recently, a microscopic evidence of a strain-enhanced ferromagnetic state was reported by Park *et al.*[10]. Using magnetic force microscopy, a ferromagnetic ground state has been confirmed for tensile-strained films, while local magnetic clusters were found for a relaxed film. Herklotz *et al.* observed that tetragonal distortion increases the magnetization in tensile-strained films. The above mentioned studies agree to some extent that the ferromagnetism in LCO is enhanced by the substrate-induced strain and that the light hole doping alone is not sufficient to produce ferromagnetism.

In this report, we present a detailed study of the structure and magnetic properties of LaCoO₃ thin films grown by pulsed laser deposition. Various substrates were used for the film growth in order to tune the strain in the epitaxial layers from tensile to compressive. All our LCO films are ferromagnetic with Curie temperatures slightly varying under different strain states. The saturated magnetic moments are much smaller than expected (theoretical) values for an excited spin-state of the Co³⁺ ions, but comparable to the previously published data. A much stronger influence of different strain states is observed on the variation of the total magnetic moments compared to changes detected in the Curie temperatures. The LCO

films grown under tensile strain have the largest magnetic moments.

2 Experiment

LaCoO₃ thin films were grown by off-axis pulsed laser deposition (KrF 248 nm) on various [001]- oriented single-crystalline substrates, i.e. SrTiO₃ (STO), LaAlO₃ (LAO), (La,Sr)(Al,Ta)O₃ (LSAT) and SrLaAlO₄ (SLAO). SiO₂ (thermally oxidized Si wafer) was used as well for depositing a thick polycrystalline LCO film. All substrates were cleaned *ex-situ* with solvents and immediately introduced into the vacuum chamber. We used stoichiometric LaCoO₃ target for depositing our films. The deposition temperature and the oxygen background pressure were 650°C and 0.45 mbar, respectively. After deposition, the films were annealed for 10 minutes at the deposition pressure and cooled down in oxygen atmosphere of 800 mbar. Thickness and deposition rate were determined from X-ray reflectivity measurements. The structure of the LCO films was characterized *ex-situ* by x-ray diffraction (XRD). The XRD measurements were carried out with a Philips X'Pert MRD diffractometer using Cu K_α radiation. For the magnetic characterization we employed SQUID magnetometry. Conductivity measurements were performed in the standard four-point geometry at temperatures between 50 and 300 K. Atomic force microscopy was employed to characterize the surface morphology and the roughness.

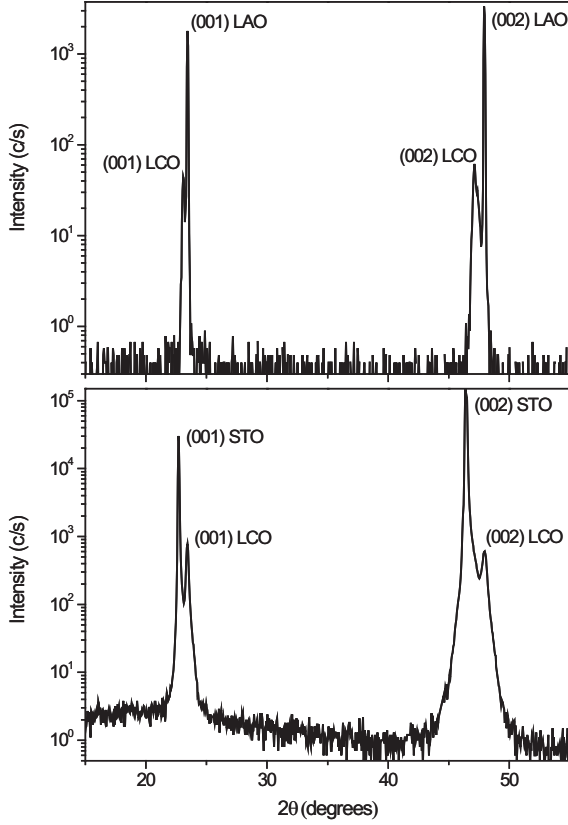


Fig. 1. $\theta-2\theta$ XRD scans of 100 nm-thick LCO films deposited on LAO (top) and STO (bottom) substrates.

3 Results

3.1 Structural characterization

In the following we discuss the structural characteristics of LaCoO₃ films grown on various substrates. Figure 1 shows $\theta-2\theta$ XRD scans of 100 nm thick LCO films deposited on (001) oriented LAO (top) and STO (bottom) single-crystalline substrates. Both films show clear (001) reflections of the pseudocubic structure. No indication of impurities or misorientation was detected. Bulk LCO, LAO and STO have the pseudocubic lattice parameters of 3.805, 3.79 and 3.905 Å, respectively, at room temperature. The lattice mismatch calculated as $(a_s - a_b)/a_s$, where a_b is

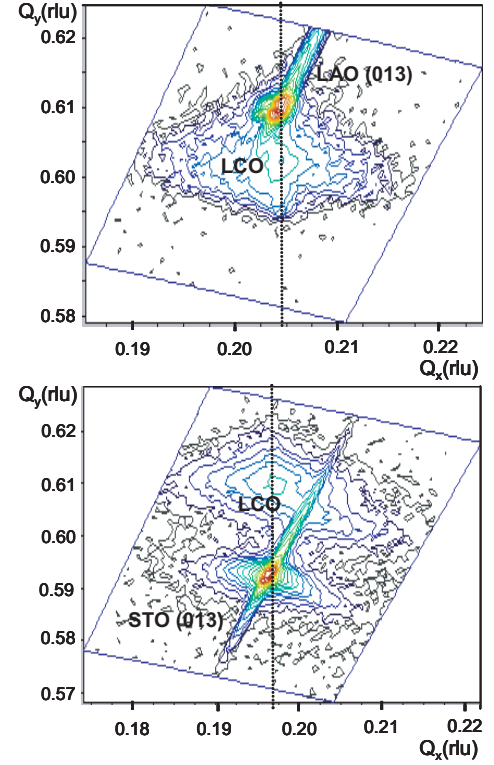


Fig. 2. XRD reciprocal space maps around the (013) reflection for a LCO/LAO film (compressive strain, top) and a LCO/STO film (tensile strain, bottom), respectively.

the pseudocubic bulk lattice parameter of LCO and a_s is the lattice parameter of the substrate is -0.4 % for LAO and +2.56 % for STO, respectively. The LCO films grow under compressive strain on LAO substrate, while on STO they experience a tensile strain. In order to obtain in-plane structural information, reciprocal space mapping (RSM) measurements around the (013) reflection were performed. The RSM results are shown in Figure 2. LCO/LAO and LCO/STO films are coherently grown, i.e. both films and the substrate have the same in-plane Q_x value. The tetragonal distortion of the films estimated as $t = 2(a - c)/(a + c)$ covers a wide range from -2% (LAO) to 2.8% (STO). The pseudocubic in-plane a and out-of-plane c lattice param-

eters and the tetragonal distortion t are listed in Table 1. The fact that 100 nm thick LCO films discussed above are fully strained in plane is surprising, taking into account that the critical thickness is less than 10 nm on these substrates [7]. The same behaviour was observed also for a LCO film grown on a LSAT substrate (see Table 1). The lattice mismatch for LCO/LSAT is 1.6%, much smaller than LCO/STO. Therefore, the LCO/LSAT film is slightly tetragonally distorted compared to LCO/STO (both grown under tensile strain).

In order to study the role played by epitaxial strain on the occurrence of ferromagnetism in LCO films we attempt also to grow relaxed LCO films. SLAO with an in-plane lattice parameter $a = 3.74 \text{ \AA}$ was chosen as a substrate for the growth of relaxed LCO films. The in-plane lattice mismatch is -1.5 %, much larger compared to LAO substrate. In figure 3 we show the results of X-ray investigation of a 100 nm thick LCO/SLAO film. The SLAO substrate has a tetragonal lattice. The LCO film adopt a pseudocubic perovskite structure. In the $\theta - 2\theta$ XRD scans (see Fig. 3a) only (001) and (002) peaks of the LCO films are visible. In-plane X-ray measurements were performed around (107) reflection of the substrate. In the RSM map shown in Fig. 3b the LCO (102) film reflection is also clearly visible, which proves the epitaxial growth of the LCO film on the tetragonal SLAO substrate. The LCO/SLAO film is almost fully relaxed, with the $a \sim c \sim 3.82 \text{ \AA}$.

In our previous report [6], we investigated the magnetic properties of LCO films grown on a piezoelectric substrate,

e.g. Pb(Mg_{1/3}Nb_{2/3})_{0.72}Ti_{0.28}O₃(001) (PMN-PT), which allows to explore directly the strain-dependent properties [12, 13, 14, 15]. The strain of the films can be reversibly and uniformly controlled by the inverse piezoelectric effect of the substrate. LCO films grown on PMN-PT substrates are partially relaxed, *i.e.* the in-plane lattice parameter of the film is different from the substrate. These films experience a tensile strain, the PMN-PT substrate having a larger pseudocubic lattice parameter, *i.e.* 4.02 \AA . The a and c lattice parameters and tetragonal distortion t of a 100 nm thick LCO/PMN-PT film are given in Table 1. From Table 1 one notices that all LCO films have an increased volume compared to the bulk unit cell, regardless of the choice of the substrate. Small angle XRR measurements show smooth and well defined interfaces between the LCO film and the single-crystalline substrates. Atomic force microscopy measurements also indicate a smooth surface morphology with a roughness (rms) ranging from 0.5 to 1 nm. We note that LCO/STO films thicker than 100 nm tend to crack, most likely caused by structural relaxation and thus the relief of tensile strain. A last remark concerning the growth, when SiO₂ was used as a substrate (not shown) the XRD spectra indicate a polycrystalline morphology of the LCO film.

3.2 Magnetic characterization

In the following the magnetic characteristics of LCO films grown on various substrates will be discussed. In order to avoid size effects we prepared films with the same thickness. All LCO films grown on single-crystalline substrates

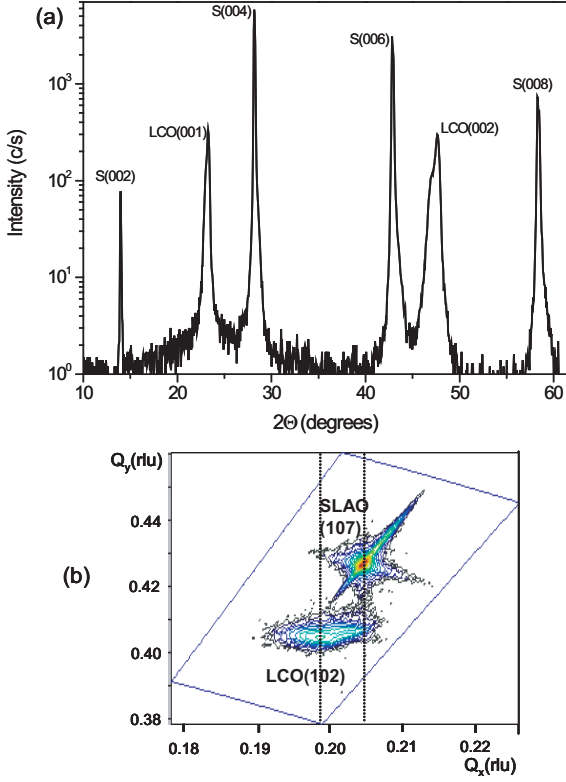


Fig. 3. (a) $\theta-2\theta$ XRD scans of 100 nm-thick LCO film deposited on SLAO substrate. (b) XRD reciprocal space map of the same film, showing the (107) reflection of the substrate and (102) reflection of the LCO film.

display ferromagnetic behaviour at low temperatures. On the contrary, when SiO₂ was employed as a substrate, no ferromagnetic order was observed down to 10 K. This indicates that polycrystalline LCO films resemble the bulk behaviour, where no magnetic order is observed. In Fig. 4 we present $M-T$ curves of 100 nm-thick LCO films grown on various substrates. Magnetization measurements were done after field cooling in a field of 200 mT applied in the film plane. Interestingly, the ferromagnetic Curie temperatures do not strongly vary for different substrates, in spite of quite different strain states. On the other hand, a

Table 1. In-plane (a) and out-of-plane (c) lattice parameters, tetragonal distortion (t) and unit cell volume ($V = a^2c$) of LCO films grown on various substrates. a_{sub} is the pseudocubic substrate lattice parameter. The unit cell volume of bulk LCO is 55.08 Å³.

LCO films (100 nm)	a_{sub} (Å)	c (Å)	a (Å)	t (%)	V (Å ³)
LCO/STO	3.905	3.785	3.896	2.8	57.45
LCO/LAO	3.79	3.85	3.789	-2	55.27
LCO/LSAT	3.87	3.804	3.867	1.6	56.88
LCO/PMN-PT	4.02	3.80	3.87	1.5	57.06
LCO/SLAO	3.74	3.81	3.82	0.2	55.59

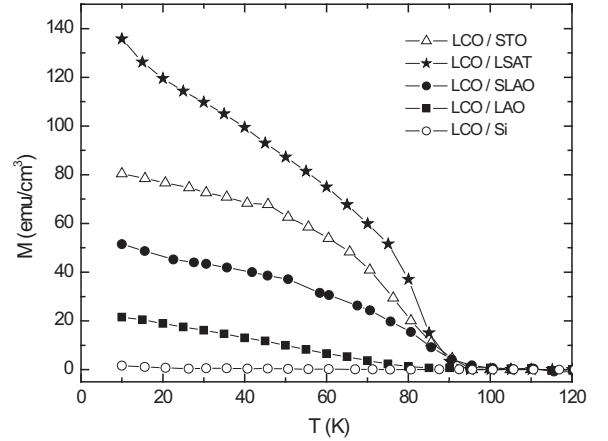


Fig. 4. Temperature dependence of the magnetization of various LCO films measured after field cooling in a field of 200 mT. The Curie temperatures are listed in Table 2.

much stronger impact of various strain states is observed on the values of the total magnetic moments. Field dependence of the magnetization was measured at 10 K for all LCO films and the total magnetic moment was estimated from the saturated magnetization. In Fig. 5 we plot a representative $M-H$ loop of a 100 nm thick LCO/LSAT

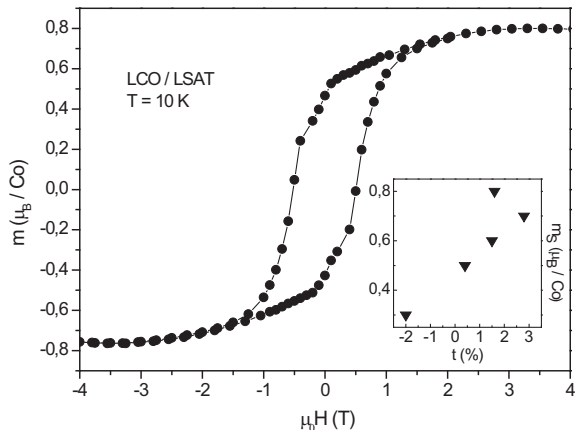


Fig. 5. Field dependence of the magnetization of 100 nm thick LCO/LSAT film measured at 10 K. Inset: variation of total magnetic moment (m_S), measured at 10 K and $\mu_0H = 5$ T, with tetragonal distortion t for various LCO films.

film. Inset shows the variation of the Co saturation magnetic moment (m_S) with the tetragonal distortion t for all LCO films. A clear correlation between m_S and t is found, *i.e.* an increase of total magnetic moment with increasing tetragonal distortion. Magnetic moments, Curie temperatures, and coercive fields of all LCO films shown in Fig. 4 are compiled in Table 2. One can notice that the values of the saturated magnetic moments of the Co³⁺ measured at 10 K in a magnetic field of 5 T are quite small. The largest values of the saturated magnetic moment were obtained for films grown under tensile strain. The highest saturation magnetization observed is approximately $0.8 \mu_B/\text{Co}$ for a LCO/LSAT film. This is a small value but still comparable to data reported in literature [5, 7]. If one assumes only a spin contribution to the magnetic moment, a value of $2 \mu_B$ (IS) and $4 \mu_B$ (HS), respectively, is expected. The relatively small values of the Co³⁺ mag-

netic moments may indicate a mixture of Co atoms in different spin states. X-ray absorption experiments which could give more insight about the Co spin state in LCO films are in progress. T_c and magnetic moments we obtained from LCO films grown under either tensile or compressive strain are comparable to the values reported in Refs. [5, 7] for similar thickness. It is interesting to notice that all films have relatively large coercive fields H_c in the range from 475 to 645 mT (see Table 2). This may indicate strong magnetocrystalline anisotropy contributions and/or domain wall pinning, which deserve further investigations. A clear bifurcation of zero-field cooling and field-cooling M - T curves is observed (not shown) in all LCO films which may indicate a glassy (ferromagnetic) state as found in bulk La _{x} Sr _{$1-x$} CoO₃, with $x \leq 0.16$ [16]. Electrical transport measurements performed between 300 K and 50 K revealed a highly insulating behaviour for all LCO films.

Despite several confirmations of ferromagnetism in LCO films from different groups, see Refs. [4, 5, 6, 8, 7], the true origin of the observed ferromagnetic state is not fully understood. Although our investigations clearly indicate that epitaxial strain plays an important role in stabilizing an excited spin-state of the Co³⁺ ions at low temperatures, some questions remain to be answered. The tetragonal distortion induced by epitaxial strain appears to be a key ingredient of ferromagnetism as confirmed also by calculations [11], where the a and c lattice parameters have been kept fixed to the experimental values reported in Refs. [4, 5]. However, the occurrence of ferromagnetism in fully re-

laxed LCO films grown on SLAO substrates having no tetragonal distortion remains puzzling. Furthermore, a T_c about 85 K has been also reported in LaCoO₃ nanoparticles, also free of distortions [17]. It is worth mentioning that a strong magnetic signal was observed in lightly-hole-doped La_{1-x}Sr_xCoO₃, x=0.002 [18], which was attributed to the formation of spin-state polarons. The authors of Ref. [18] found that holes introduced in the low spin state of LaCoO₃ by substitution of Sr²⁺ for La³⁺ transform the six nearest neighboring Co³⁺ ions to the intermediate spin state forming octahedrally shaped spin-state polarons. These spin-state polarons behave like magnetic nanoparticles embedded in an insulating nonmagnetic matrix. The role of light hole doping due to oxygen vacancies on the ferromagnetism in LaCoO₃ films can't be totally ruled out. However, our previous investigations [6] of LCO films deposited on piezoelectric substrate under tensile strain clearly show that the magnetization decreases with the reversible release of tensile strain below T_c . Using this approach, *e.g.* reversible control of the strain by the inverse piezoelectric effect of the substrate, one can overcome the effect of other parameters, *e.g.* oxygen nonstoichiometry. The increased volume observed in all LCO films prepared on different substrates is consistent with the occurrence of an excited state of Co³⁺ ions. The ionic radius of low-spin LS Co³⁺ (0.545 Å) is smaller than that of high-spin HS Co³⁺ (0.61 Å) [19]. Finally, we note that the highly insulating behaviour shown by all LCO films indicates that the ferromagnetic coupling mechanism is different from Sr-doped La_{1-x}Sr_xCoO₃ unless the ferro-

Table 2. Magnetic moment (m_S) at 10 K, Curie temperature (T_C), and coercive field (H_C) of LCO films grown on different substrates.

LCO films (100 nm)	m_S (μ_B /f.u.)	T_C (K)	H_C (mT)
LCO/STO	0.7	86	344
LCO/LAO	0.3	75	475
LCO/LSAT	0.8	85	560
LCO/PMN-PT	0.6	87	430
LCO/SLAO	0.5	84	645

magnetism is not long-range, but occurs in isolated clusters.

4 Summary

To summarize, we have studied the influence of various strain states on the magnetic properties of LaCoO₃ thin films. Single-phase (001) oriented LaCoO₃ layers were grown on all substrates despite large misfits, with tetragonal distortion varying from -2% to 2.8%. All LaCoO₃ films are ferromagnetic at low temperatures, contrary to the bulk. The Curie temperature shows little variation with different strain states. We observed an increase of Co saturation magnetic moment with increasing tetragonal distortion. This result confirms that tetragonal distortion plays an important role in the occurrence of ferromagnetism in LaCoO₃ thin films.

We would like to thank T. Kroll, D. Fuchs and K. Nenkov for discussions and useful suggestions. This work was supported by Deutsche Forschungsgemeinschaft, FOR 520.

References

1. M. Imada, A. Fujimori, and Y. Tokura, *Rev. Mod. Phys.* **70**, 1039 (1998).
2. L. Craco and E. Müller-Hartmann, *Rev. Rev. B* **77**, 045130 (2008).
3. L. Hozoi, U. Birkenheuer, H. Stoll, and P. Fulde, *New Journal of Physics* **11**, 023023 (2009).
4. D. Fuchs, C. Pinta, T. Schwarz, P. Schweiss, P. Nagel, S. Schuppler, R. Schneider, M. Merz, G. Roth, and H. v. Löhneysen, *Phys. Rev. B* **75**, 144402 (2007).
5. D. Fuchs, E. Arac, C. Pinta, S. Schuppler, R. Schneider, and H. v. Löhneysen, *Rev. Rev. B* **77**, 014434 (2008).
6. A. Herklotz, A. D. Rata, L. Schultz, and K. Dörr, *Phys. Rev. B* **79**, 092409 (2009).
7. Virat Vasav Mehta, Marco Liberati, Franklin J. Wong, Rajesh Vilas Chopdekar, Elke Arenholz, and Yuri Suzuki, *Journal App. Phys.* **105**, 07E503 (2009).
8. J. W. Freeland, J. X. Ma, J. Shi, *Appl. Phys. Lett.* **93**, 212501 (2008)
9. J. M. Rondinelli and N. A. Spaldin, *Rev. Rev. B* **79**, 054409 (2009).
10. S. Park, P. Ryan, E. Karapetrova, J. W. Kim, J. X. Ma, J. Shi, J. W. Freeland, and Weida Wu, *Appl. Phys. Lett.* **95**, 072508 (2009).
11. Kapil Gupta and Priya Mahadevan *Rev. Rev. B* **79**, 020406(R) (2009).
12. K. Dörr, O. Bilani-Zeneli, A. Herklotz, A. D. Rata, K. Boldyreva, J. -W. Kim, M. C. Dekker, K. Nenkov, L. Schultz, and M. Reibold, *Eur. Phys. J. B* **71** 361 (2009).
13. A. D. Rata, A. Herklotz, K. Nenkov, L. Schultz, and K. Dörr, *Phys. Rev. Lett.* **100**, 076401 (2008).
14. O. Bilani-Zeneli, A. D. Rata, A. Herklotz, O. Mieth, L. M. Eng, L. Schultz, M. D. Biegalski, H. M. Christen, and K. Drr, *J. Appl. Phys.* **104**, 054108 (2008).
15. M. C. Dekker, A. D. Rata, K. Boldyreva, S. Oswald, L. Schultz, and K. Dörr, *Rev. Rev. B* **80**, 144402 (2009).
16. J. Wu, H. Zheng, J. F. Mitchell, and C. Leighton, *Rev. B* **73**, 020404(R) (2006).
17. I. Fita, V. Markovich, D. Mogilyansky, R. Puzniak, A. Wisniewski, L. Titelman, L. Vradman, M. Herskowitz, V. N. Varyukhin, and G. Gorodetsky *Phys. Rev. B* **77**, 224421 (2008).
18. A. Podlesnyak, M. Russina, A. Furrer, A. Alfonsov, E. Vavilova, V. Kataev, B. Buchner, Th. Strassle, E. Pomjakushina, K. Conder, and D. I. Khomskii, *Rev. Rev. Lett.* **101**, 247603 (2008).
19. R. D. Shannon and C. T. Prewitt, *Acta Crystallogr., Sect. B: Struct. Crystallogr. Cryst. Chem.* **25**, 925 (1969).